Heat and Mass Transfer 39 (2003) 223–230
DOI 10.1007/s00231-002-0301-3

# Heat and mass transfer with phase change in a rectangular enclosure packed with unsaturated porous material

**W. Liu, X.M. Huang, S.B. Riffat**



**Abstract** The paper has presented a seven-field mathematical model with ten variables to describe the simultaneous heat and mass transfer with phase change in the unsaturated porous medium that is enclosed in a rectangular enclosure. Both liquid and vapor migration in the porous matrix are evaluated at the same time, and gaseous bulk motion is simulated numerically. The numerical results are discussed with emphasis on the effect of evaporation and condensation of *R113* in the vertical enclosure, which may have an application in the room passive heating for the buildings in winter. As solar energy or low-grade waste heat could be used if the enclosure is adequately designed to transfer heat from the outside to the room of the building, the present method may be propitious to the energy conservation. Aimed to this purpose, the heat transfer character of the enclosure is analyzed for the change of *Nu* number with different *Ra* number and *Da* number.

**Nomenclature**

| | |
|---|---|
| $A$ | aspect ratio |
| $c$ | specific heat, $J/(Kg{\cdot}K)$ |
| $D_a$ | Darcy number |
| $D_l$ | diffusivity of liquid in porous medium, $m^2/s$ |
| $D_v$ | molecular diffusivity of vapor in air, $m^2/s$ |
| $D_{Tv}$ | diffusivity due to exist of temperature gradient, $m^2/(s{\cdot}K)$ |
| $D_{lv}$ | diffusivity due to exist of moist content gradient, $m^2/s$ |
| $F_O$ | Fourier number |
| $g$ | acceleration of gravity, $m/s^2$ |
| $H$ | vertical height in y-direction of soil bed, $m$ |
| $\vec{j}$ | unit vector |
| $J_a$ | factor of phase change, dimensionless number |
| $k_g$ | equivalent permeability of gas-mixture, $m^2$ |
| $k_l$ | unsaturated permeability of liquid, $m^2$ |
| $K_g$ | infiltrating conductivity of gas-mixture, $m/s$ |
| $K_l$ | hydraulic conductivity of liquid, $m/s$ |
| $L$ | horizontal width in x-direction of porous bed, $m$ |
| $Le$ | Lewis number |
| $\dot{m}$ | mass rate of phase change, $Kg/(m^3{\cdot}s)$ |
| $Nu_h$ | Nusselt number defined in Eq. (27) |
| $P$ | pressure, $Pa$ |
| Pr | Prandtl number |
| $Ra$ | Rayleigh number |
| $S$ | source term, saturation |
| $t$ | time, $s$ |
| $T$ | temperature, $K$ (°C) |
| $u$ | velocity component in x-direction, $m/s$ |
| $v$ | velocity component in y-direction, $m/s$ |
| $V$ | averaging volume, $m^3$ |
| $\vec{V}$ | velocity vector, $m/s$ |
| $\vec{V}_{v,d}$ | vapor diffusivity velocity |

**Greek symbols**

| | |
|---|---|
| $\alpha$ | thermal diffusivity of fluid |
| $\alpha_m$ | thermal diffusivity of porous media |
| $\beta$ | thermal expansion coefficient, $1/K$ |
| $\gamma$ | latent heat, $J/Kg$ |
| $\Gamma_D$ | dimensionless number |
| $\varepsilon$ | phase content, % |
| $\lambda_m$ | apparent thermal conductivity, $W/(m{\cdot}K)$ |
| $\lambda$ | thermal conductivityn, $W/(m{\cdot}K)$ |
| $\Theta$ | dimensionless temperature |
| $\Lambda$ | dimensionless conductivity |
| $\mu$ | viscosity, $Kg/(m{\cdot}s)$ |
| $\upsilon$ | kinematic viscosity, $m^2/s$ |
| $\rho$ | density, $Kg/(m^3$ |
| $\varphi$ | dimensionless parameter |
| $\Phi$ | dimensionless parameter |
| $\omega$ | porosity, % |

**Subscripts**

| | |
|---|---|
| $a$ | air, ambient |
| $c$ | cold wall |
| $eff$ | effective quantities |
| $g$ | gaseous mixture |
| $h$ | hot wall |
| $l$ | liquid |
| $m$ | apparent mean, mass |
| $s$ | solid |
| $v$ | vapor |

*Received: 10 May 2001*
*Published online: 15 June 2002*


W. Liu (✉), X.M. Huang
Department of Power Engineering,
Huazhong University of Science and Technology,
Wuhan 430074, P.R. China
E-mail: weiliu@public.wh.hb.cn

S.B. Riffat
School of the Built Environment, The University of Nottingham,
University Park, Nottingham NG7 2RD, UK

The current work is financially supported by the National Key Fundamental Research Development Program of China (No.G2000026303), the National Natural Science Foundation of China (No.59976010) and the Doctoral Foundation of Education Ministry of China (No.2000048731).

**Superscript**

$\sim$ dimensionless quantities

## 1 Introduction

It is well known that the porous materials are widely used or exist in many aspects of engineering, agriculture and environment protection. To name a few, applied examples include thermal insulation in buildings, heat pipe system coupled with earth heat source, convective drying for food and agricultural products, heat and moisture migration in soil, ground environment for crop growth, disposal of thermal, chemical and nuclear wasters, and so on. In this paper, attention has been paid to the energy conservation in the buildings, which may result in an important energy saving technique to yield a substantial heating or air-conditioning effect for the room.



Since many physical mechanisms on transport process are involved in the liquid-unsaturated porous materials, the theoretical modeling for simultaneous migration of heat, moisture and gas cannot be conducted easily. In view of the complexity of multi-phase flow and phase change process, the volume-averaging method to solve the problem was developed by Slattery [1] and Whitaker [2]. Those are very different from the well-done work by Philip & DeVries [3] and De Vries [4] based on the thermodynamics principle just involving a few physical quantities, like temperature, moisture content and pressure. Some further investigations had been conducted by Udell [5], Vafai [6], Cheng [7] and Gray [8] to analyze various phenomena that were dealing with heat and mass transfer and liquid infiltrating phenomena in saturated or unsaturated problems, which highly contribute the substantial improvements to theoretical modeling and experimental setting up. Very recently, the study on unsaturated porous materials in the soil medium was reported by references [9, 10]. In those papers the authors made great efforts to perfect the theoretical model and experiment measures. Bouddour *et al.* presented a new mathematical model for heat and mass transfer in porous media [9] and tried to take all the complexity of interactions into account, involved by the coupled heat and mass transfer in porous media. He used the method of multiple scale expansions to upscale description at the pore scale to the macroscopic scale. But it seems the mathematical model is too complex to be solved. Some researchers concentrate their attention on the experiment study of buoyancy-induced flow of water with phase-change heat transfer in porous media heated by a rather large heat flux [10, 11], however, for the phase change at relatively low temperature in porous media there exists few references. Other researchers are interested in the phenomena that depart from local thermal equilibrium [12]. In Perré and Turner's paper they show a 3-D drying model [13]. Significant work [14, 15] aimed to analyze the effect of ambient parameters on all field variables was well done in the confined soil bed with profiling all variable distributions in two dimension, influenced by the ambient conditions changing with time.

In the previous study for an unsaturated bed packed with porous material [16, 17], we presented two kinds of free cooling surfaces, horizontal and vertical, with a variety of ambient conditions. Some physical quantities in the form of two-dimension field had been simulated with an opening system. As the working medium was water, the evaporating porous bed gave rise to no problems to the environment, and it could be adopted in the case of free evaporative cooling. But in the case of passive heating for room building utilizing natural energy of low grade like solar energy, we choose an enclosed porous bed filled with working medium, *R113* or *R30*, at the phase-change temperature 30–60 °C depended on pressure. In the present design the heat flux transfers in the direction from the outside to the inside of room (see Fig. 1), for it can absorb heat from solar energy in the high temperature region and release it in the low temperature region of room side duo to evaporation and condensation. To testify the performance of heat-flux migration in the enclosure, the surface characters on heat transfer are analyzed via the change of *Nu* number with different *Ra* number and *Da* number. Such a concept of room heating by controlling the direction of heat flow may provide a possible application in the actual building engineering based on the theoretical work conducted by the current study.

## 2

### 2.1 Theoretical modeling

We have established a seven-field model [16] to describe the simultaneous heat, moisture and vapor migration in unsaturated porous media with phase change. The field variables include temperature $T$, liquid content $\varepsilon_l$, pressure $P$, liquid velocity $\vec{V}_l$, gas velocity $\vec{V}_g$, vapor velocity $\vec{V}_v$ and phase-change rate of evaporation and condensation $\dot{m}$. For the two dimensional fields, we have $\vec{V}_l = u_l\vec{i} + v_l\vec{j}$, $\vec{V}_g = u_g\vec{i} + v_g\vec{j}$, $\vec{V}_v = u_v\vec{i} + v_v\vec{j}$, which means the set of equations currently considered has ten variables to be solved.

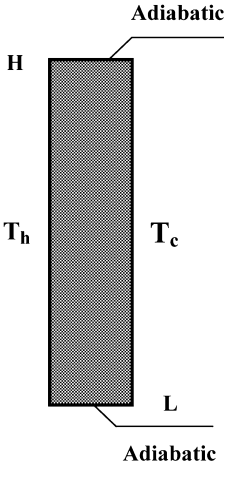


**Fig. 1.** Physical model of porous packed bed

**Continuity equations**

$$\text{Liquid: } \frac{\partial(\varepsilon_l\rho_l)}{\partial t} + \nabla\cdot(\varepsilon_l\rho_l\vec{V}_l) = -\dot{m} \tag{1}$$

$$\text{Gas: } \frac{\partial(\varepsilon_g\rho_g)}{\partial t} + \nabla\cdot(\varepsilon_g\rho_g\vec{V}_g) = \dot{m} \tag{2}$$

$$\text{Vapor: } \frac{\partial(\varepsilon_g\rho_v)}{\partial t} + \nabla\cdot(\varepsilon_g\rho_v\vec{V}_v) = \dot{m} \tag{3}$$

**Momentum equations**

$$\text{Liquid phase: } \frac{\partial\vec{V}_l}{\partial t} + \vec{V}_l\cdot\nabla\vec{V}_l - \frac{\dot{m}}{\varepsilon_l\rho_l}\vec{V}_l = -\frac{gD_l}{K_l}\nabla\varepsilon_l - \frac{g\varepsilon_l}{K_l}\vec{V}_l - \frac{g\varepsilon_g}{K_g}(\vec{V}_l - \vec{V}_g) - \vec{g} + \nu_l\nabla^2\vec{V}_l \tag{4}$$

Gaseous phase:

$$\frac{\partial\vec{V}_g}{\partial t} + \vec{V}_g\cdot\nabla\vec{V}_g + \frac{\dot{m}}{\varepsilon_g\rho_g}\vec{V}_g = -\frac{1}{\rho_g}\nabla p - \frac{g\varepsilon_g}{K_g}(\vec{V}_g - \vec{V}_l) - \vec{g}\beta(T - T_c) + \nu_g\nabla^2\vec{V}_g \tag{5}$$

**Energy equation**

$$(\rho c)_m\frac{\partial T}{\partial t} + \left((\rho c)_l\vec{V}_l + (\rho c)_g\vec{V}_g + (\rho c)_v\overrightarrow{V}_v\right)\cdot\nabla T + \left((\rho c)_l\vec{V}_l\cdot\nabla\varepsilon_l + (\rho c)_g\vec{V}_g\cdot\nabla\varepsilon_g + (\rho c)_v\overrightarrow{V}_v\cdot\nabla\varepsilon_g\right)T = \lambda_m\nabla^2 T - \dot{m}\gamma + S \tag{6}$$

## 2.2 Model discussions

For the above partial differential equations, some of the characteristics for the theoretical modeling could be discussed as follows.

(1) As one of the seven-field quantities, the absolute velocity of vapor (*R113* in this paper) can be defined as $\vec{V}_v = \vec{V}_g + \vec{V}_{v,d}$, and the vapor diffusivity velocity can be indicated as $\vec{V}_{v,d} = -D_{Tv}\nabla T - D_{lv}\nabla\varepsilon_l$ [16]. When the quantification relation among diffusivity velocity, temperature and phase content are established, we can easily explain the effect of vapor diffusivity on the equilibrium of mass and energy. Thus the continuity equation (3) can be taken as a supplement relation contributed to the present model, and the absolute velocity of vapor plays an important role to the temperature level in the energy equation. This may also be the good way of adding the micro-mechanism of the molecular diffusivity into the macro-motion of gaseous phase, through relative relation between $\vec{V}_v$ and $\vec{V}_g$ that also appears in the momentum equation.

(2) In the modeling assumptions, the Dalton's partial pressure law $P = P_a + P_v$ is introduced ($P_a$ for air partial pressure and $P_v$ for saturated vapor pressure) and the volume-content relation of $\varepsilon_a = \varepsilon_v = \varepsilon_g$ for air and vapor are satisfied (air and vapor are filled everywhere in the pore-space of porous medius). Thus we can reasonably regard that $\varepsilon_a$ and $\varepsilon_v$ are not independent variables, as $\varepsilon_g$ is depended on $\varepsilon_l$ which is the only content-indepentent variable. This treatment may be the key point for us to solve the problem by reducing the variables numbers in the equations.

(3) Based on the fact $\varepsilon = \varepsilon_s + \varepsilon_l + \varepsilon_g$, the mean physical properties of porous media can be written as $(\rho c)_m = \varepsilon_s(\rho c)_s + \varepsilon_l(\rho c)_l + \varepsilon_g(\rho c)_g$. And from the principle of constant volume content for gaseous components $\varepsilon_g = \varepsilon_a = \varepsilon_v$, we simply set $(\rho c)_g = \rho_a c_a + \rho_v c_v$. The apparent heat conductivity of the porous material, according to the mean-weighted method, is simply defined as $\lambda_m = \varepsilon_s\lambda_s + \varepsilon_l\lambda_l + \varepsilon_g\lambda_g$.

(4) From above discussions (1–3), we could say that two kinds of physical states (liquid and vapor) and motion manners (macro-motion and micro-diffusivity) for the moisture in the unsaturated porous material are both considered in the mathematical modeling. And both of motion rate and phase-change rate for moisture are taken into account.

(5) Noting that $K_l = k_l g/\upsilon_l$ and $K_g = k_g g/\upsilon_g$, we had developed an effective formulation to calculate the gaseous infiltrating conductivity $K_g$ [17] corresponding to the liquid hydraulic conductivity $K_l$, which can demonstrate the mechanisms of Darcy's drag resistance in terms of gaseous phase and the reaction of liquid to gaseous mixture. It may be rarely considered by others and could be written as

$$K_g = (1-S)^3\left(\frac{1-ga}{1-ga(1-S)}\right)^{4/3}\frac{\upsilon_l}{\upsilon_g}K_l \tag{7}$$

Through such a disposal, we can overcome the difficulty lacking of physical property in the gaseous momentum equation, and get reasonable calculation results benefiting from this. Furthermore, it allows us to consider the relative motion between gas and liquid phases by the Darcy's terms both in gas and liquid momentum equations (4–5).

(6) As we assume that the vapor (water, *R113*, or other refrigerants) in the interstitial space is of the saturated pressure, so that the present model is developed to reflect the evaporation and the condensation in the porous matrix. As a mater of fact, the phase change in the unsaturated porous material acts as an evaporation source some time or a condensation sink some other time, or both of source and sink at the same time at different regions. The sign of field variable $\dot{m}$ could represent the characteristic of source or sink. The contribution of phase change rate $\dot{m}$ has been added into the mass, momentum and energy equations.

From the above discussions, we have explained the present ten-variable equations, in which the momentum equations are very analogous to Navier-Stokes equation, but very different from the Darcy's motion equation. By adding the following expression as a supplemental relation for the model, the equations (1–6) can be perfected mathematically.

$$\vec{V}_v = \vec{V}_g + \vec{V}_{v,d} = \vec{V}_g - D_{Tv}\nabla T - D_{lv}\nabla\varepsilon_l \tag{8}$$

There should be no doubts that the mathematical model under investigation introduces more transport or migration mechanisms in the porous packed bed compared with some other models or with our previous study, which improves our theoretical modeling [14–17] both mathematically and physically.



## 3 Model simplification and non-dimensionless

Some basic assumptions have been made in the present case of investigation.

(1) Local thermal equilibrium is satisfied throughout the porous media.
(2) Gaseous mixture (air plus vapor) in the enclosure can be treated as ideal gas.
(3) Partial pressure of vapor is in the equilibrium pressure of saturated state.
(4) Boussinesq's approximation is suitable for natural convection in gaseous space.
(5) Momentum change rate of liquid is so small that it could be omitted.

### 3.1 Dimensionless equations [18]

To simplify the controlling equations, the dimensionless quantities should be defined firstly.

$$\Theta = \frac{T - T_c}{T_h - T_c}, \quad \tilde{P} = \frac{k_g}{\alpha_m \rho_g \upsilon_g} P, \quad \tilde{V}_l = \frac{L}{\alpha_m}\vec{V}_l,$$

$$\tilde{V}_g = \frac{L}{\alpha_m}\vec{V}_g, \quad \tilde{V}_v = \frac{L}{\alpha_m}\vec{V}_v, \quad \tilde{m} = \frac{L^2}{\alpha_m}\dot{m}$$

$$Fo = \frac{\alpha_m}{L^2}t, \quad Da = \frac{k_g}{L^2}, \quad Ra = \frac{g\beta\Delta T L^3}{\alpha_m \upsilon_g},$$

$$\mathrm{Pr} = \frac{\upsilon_g}{\alpha_m}, \quad Le^* = \frac{\alpha_m}{D_{Tv}}\Delta T, \quad Le^{**} = \frac{\alpha_m}{D_{lv}}, \quad \Lambda = \frac{\lambda_g}{\lambda_m}$$

$$\varphi = \frac{\varepsilon_g K_l}{\varepsilon_l K_g}, \quad \Gamma_D = \frac{D_l}{\alpha_m}, \quad \tilde{g} = \frac{H^3}{\upsilon_l \alpha_m}\vec{g},$$

$$Ja = \frac{\gamma}{c}\Delta T, \quad \phi_l = \frac{(\rho c)_l}{(\rho c)_m}, \quad \phi_g = \frac{(\rho c)_g}{(\rho c)_m}, \quad \phi_v = \frac{(\rho c)_v}{(\rho c)_m}$$

**Continuity equations**

$$\text{Liquid: } \frac{\partial(\varepsilon_l\tilde{\rho}_l)}{\partial Fo} + \nabla(\varepsilon_l\tilde{\rho}_l\tilde{V}_l) = -\tilde{m} \tag{9}$$

$$\text{Gas: } \frac{\partial(\varepsilon_g\tilde{\rho}_g)}{\partial Fo} + \nabla(\varepsilon_g\tilde{\rho}_g\tilde{V}_g) = \tilde{m} \tag{10}$$

$$\text{Vapor: } \frac{\partial(\varepsilon_g\tilde{\rho}_v)}{\partial Fo} + \nabla(\varepsilon_g\tilde{\rho}_v\tilde{V}_v) = \tilde{m} \tag{11}$$

**Momentum equations**

$$\text{Liquid phase: } (1+\varphi)\tilde{V}_l = -\frac{\Gamma_D}{\varepsilon_l}\nabla\varepsilon_l + \varphi\tilde{V}_g - \frac{Da}{\varepsilon_l}\tilde{g} \tag{12}$$

$$\text{Gaseous phase: } \frac{D_a}{\mathrm{Pr}}\left(\frac{\partial\tilde{V}_g}{\partial Fo} + \tilde{V}_g\cdot\nabla\tilde{V}_g\right) = -\nabla\tilde{P} - \varepsilon_g(\tilde{V}_g - \tilde{V}_l) - RaDa\Theta\vec{j} + Da\nabla^2\tilde{V}_g \tag{13}$$

**Energy equation**

$$\frac{\partial\Theta}{\partial Fo} + (\phi_l\tilde{V}_l + \phi_g\tilde{V}_g + \phi_v\tilde{V}_v)\cdot\nabla\Theta + (\phi_l\tilde{V}_l\cdot\nabla\varepsilon_l + \phi_g\tilde{V}_g\cdot\nabla\varepsilon_g + \phi_v\tilde{V}_v\cdot\nabla\varepsilon_g)\Theta = \nabla^2\Theta - Ja\tilde{m} \tag{14}$$

If not involving the relative relations between the liquid and the gas phases, all steady-state continuity, momentum and energy equations without Soret effect become

$$\nabla(\varepsilon_l\tilde{\rho}_l\tilde{V}_l) = -\tilde{m} \tag{15}$$

$$\nabla(\varepsilon_g\tilde{\rho}_g\tilde{V}_g) = \tilde{m} \tag{16}$$

$$\nabla(\varepsilon_g\tilde{\rho}_v\tilde{V}_v) = \tilde{m} \tag{17}$$

$$\tilde{V}_l = -\frac{\Gamma_D}{\varepsilon_l}\nabla\varepsilon_l - \frac{Da}{\varepsilon_l}\tilde{g} \tag{18}$$

$$\tilde{V}_g\cdot\nabla\tilde{V}_g = -\frac{\mathrm{Pr}}{Da}\nabla\tilde{P} - \frac{\mathrm{Pr}}{Da}\varepsilon_g\tilde{V}_g - Ra\mathrm{Pr}\Theta\vec{j} + \mathrm{Pr}\nabla^2\tilde{V}_g \tag{19}$$

$$(\phi_l\tilde{V}_l + \phi_g\tilde{V}_g + \phi_v\tilde{V}_v)\cdot\nabla\Theta = \nabla^2\Theta - Ja\tilde{m} \tag{20}$$

Where the dimensionless equation of vapor diffusivity take the form as

$$\tilde{V}_{v,d} = -\nabla\Theta/Le^* - \nabla\varepsilon/Le^{**} \tag{21}$$

As one can see from equations (15–20), we have exerted some concrete simplification on equations (1–6), by which the numerical calculation is relatively easy to carry out.

### 3.2 Boundary conditions

The initial and boundary conditions to solve the controlling equations are set according to the physical model shown in Fig. 1. The hot and cold temperatures $T_h$ and $T_c$ are specified over the left and the right vertical surfaces. The upper and underlying sides are subjected to the boundary condition of heat insulation. All of the four surfaces are considered as the moisture-insulation boundaries.

$$X = 0 \quad \Theta = 1 \quad \tilde{V}_g = \tilde{V}_l = 0 \tag{22}$$

$$X = 1 \quad \Theta = 0 \quad \tilde{V}_g = \tilde{V}_l = 0 \tag{23}$$

$$Y = 0 \quad \frac{\partial \Theta}{\partial Y} = 0 \quad \tilde{V}_g = \tilde{V}_l = 0 \tag{24}$$

$$Y = 1 \quad \frac{\partial \Theta}{\partial Y} = 0 \quad \tilde{V}_g = \tilde{V}_l = 0 \tag{25}$$

$$t = 0 \quad \Theta(X, Y, t) = 0 \tag{26}$$

## 4
## Analysis and discussion

The governing equations (15–20) together with the boundary conditions mentioned above are solved with the finite difference method. Noting that the pressure changes in transport process and heat and mass transfer are highly coupled, the pressure-based algorithm is principally used in the numerical formulations and computations with treating staggered grid in primitive variables and *ADI* technique is adopted to solve the coupled linear equations. Since there exists no pressure-related terms in liquid-phase momentum equation, the pressure correction equations are needed to develop through gas-mixture continuity equation (16) only for gas momentum equation. In order to ensure the convergence of calculating procedure, some technical treatments like under relaxation and error feedback are adopted.

The similar transport analysis and calculation was made for the porous bed with a horizontal or vertical free cooling surface in our previous study. There exists a big driving potential for mass migration with a strong evaporation on the surface opened to the environment, and at the bottom the solid matrix is saturated with liquid. Therefore, the liquid-phase content changes obviously along the altitude direction of the porous bed with a relatively larger content gradient. In such case, the coupling of numerical calculation for the model can be carried out with less difficulty. Whereas, for the mass migration occurring in a porous enclosure, there is no suction force from the surface evaporation, the driving potential for the liquid movement mainly depends on the capillary head inside the bed. In this case, the liquid content field changes a little, and the choosing of the relaxation factor is rather important during the calculation process, in other words, the coupling calculation is some difficult to be conducted.

To discuss the influences of various control parameters on heat and mass transfer, we made the calculation for the present model numerically under different *Ra* and *Da* numbers. The results are analyzed as follows.

### 4.1
### The flow and heat transfer patterns

The patterns of isotherm line and streamline and the contours of evaporation or condensation rate for a wide range of $Ra^{\star} = \Lambda Ra$ are separately shown from Fig. 2 to Fig. 4 with the basic calculating parameters fixed as: Darcy number $Da = 10^{-4}$, aspect ratio $A=H/L=5$, prescribed cold wall temperature $T_c = 290$K, side-to-side temperature difference $\Delta T=30$ °C.

The flow of gaseous mixture for rather low $Ra^{\star}$ number is illustrated in Fig. 3(a–b). The value of dimensionless stream function is very small compared with the cases shown in Fig. 3(c–e), which demonstrates that the flow in the enclosure is very weak, and the patterns of streamline are almost symmetrical along the line $L/2$. The isotherm patterns in Fig. 2(a–b) are similar to that dominated by conduction, but there exist a little evaporation and condensation just in the regions near the warm wall and the cold wall, as shown in Fig. 4(a–b).

With increase in $Ra^{\star}$ number, see Fig. 2(c–e), the isotherm lines are apart from the symmetry. Along the vertical direction the temperature drops obviously from the top to the bottom. The patterns of evaporation and condensation fields change a lot, and the rates of phase change increase, as shown in Fig. 4(c–e).

When the $Ra^{\star}$ number becomes higher, see Figs. 2 and 3(c–e), the streamline pattern apparently deviates from the symmetry and the value is dramatically raised at the same time. Then the isotherm lines are twisted. These phenomena manifest the flow in the enclosure is becoming stronger and stronger. And when the $Ra^{\star}$ number approaches $10^8$, there will be a thermal parallel flow in the core region of the enclosure.

As shown in Fig. 4(a–e), the evaporation occurs in the left-down region, and the condensation occurs in the upper-right region, while the $Ra^{\star}$ number becomes bigger and bigger. Those phenomena may imply that the phase change in unsaturated porous media is not only associated with the Darcy's drag resistance, but also related to the gravitational and the capillary mechanisms.

### 4.2
### The ability of heat transfer

To check the heat transfer capability of the enclosure with unsaturated porous media we define a dimensionless average Nusselt number $Nu_h$ as:

$$Nu_h = \frac{\frac{1}{A}\int_0^A -\lambda_m \frac{\partial \Theta}{\partial X}\big|_{X=0} dY}{\lambda_m(\Theta_h - \Theta_c)} \tag{27}$$

Where $\Theta_h$ and $\Theta_c$ are the dimensionless temperatures for the warm wall and the cold wall respectively, and $\lambda_m$ is the mean apparent heat conductivity. This number indicates that the proportion of the rate of heat transfer through porous media to that of pure conduction.

Observing Figs. 5 and 6, we can find that when the product $Ra^{\star}Da < 100$, neither $Ra^{\star}$ number nor *Da* number will produce any effect on $Nu_h$ number. However, once the product is bigger than 100 the increase of either of *Ra* number and *Da* number can cause some increase to $Nu_h$ number. The flow at this time is toward to a pattern like boundary layer, which is a fully developed one. The slope of curve in Fig. 6 increases with the rise of *Da* number at first. However, when *Da* number increases further, the slope decreases. According to these characters of the $Nu_h$ distribution, we can divide the flow field into three regimes. The first one is conduction regime. In this regime the natural convection hasn't been formed or it is still very weak. As the results, $Nu_h$ number keeps constant or

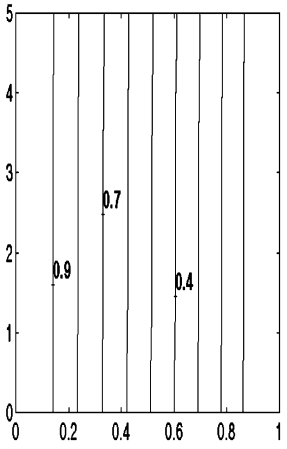


(a) Λ Ra=$10^4$, Da=$10^{-4}$

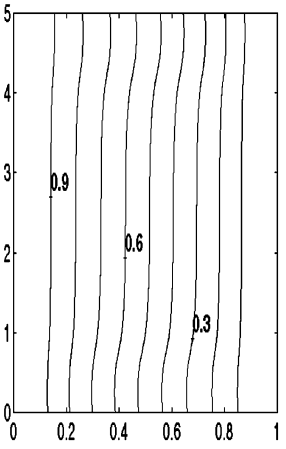


(b) Λ Ra=$10^5$, Da=$10^{-4}$

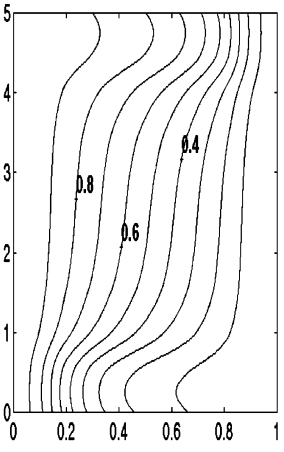


(c) Λ Ra=$10^6$, Da=$10^{-4}$

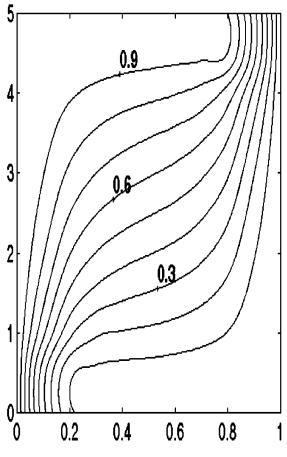


(d) Λ Ra=$10^7$, Da=$10^{-4}$

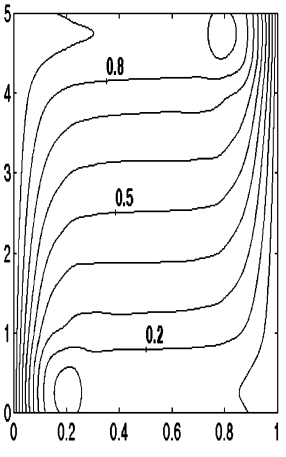


(e) Λ Ra=$10^8$, Da=$10^{-4}$

**Fig. 2.** Isotherm for different *Ra* number

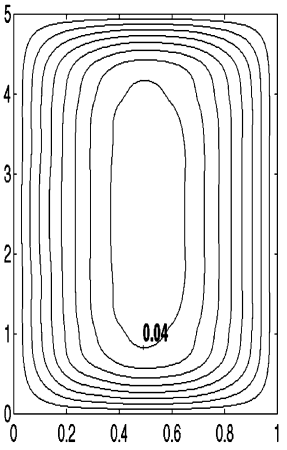


(a) Λ Ra=$10^4$, Da=$10^{-4}$

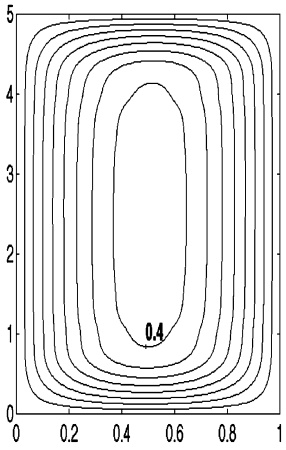


(b) Λ Ra=$10^5$, Da=$10^{-4}$

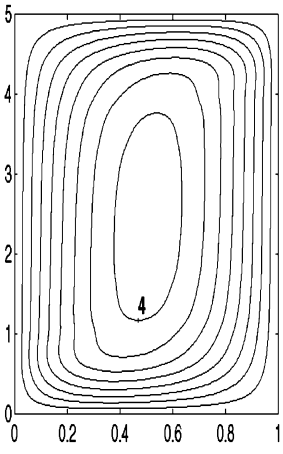


(c) Λ Ra=$10^6$, Da=$10^{-4}$

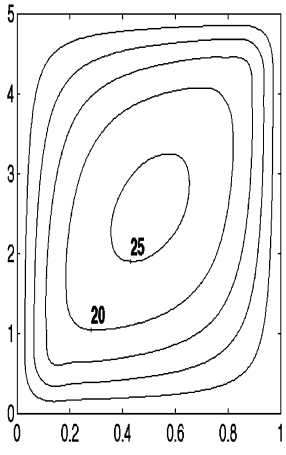


(d) Λ Ra=$10^7$, Da=$10^{-4}$

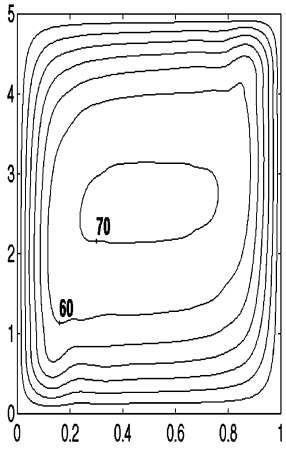


(e) Λ Ra=$10^8$, Da=$10^{-4}$

**Fig. 3.** Gas flow for different *Ra* number

changes very little. The second one is strongly Darcy-induced regime where the rate of heat transfer increases greatly with the increase in *Da* number at a certain *Ra* number. The third one is weakly Darcy-induced regime. The Darcy mechanism in this regime is no longer one of the key influence factors for the rate of heat transfer, as in this case the influence of *Da* number on $Nu_h$ number is extremely little. For higher *Ra* number, the *Da* number is relatively small for the flow to reach *Da*-unchanged regime. On the other hand the buoyancy affects the flow greatly, as it is intensive when *Ra* number increases with strengthening heat transfer.

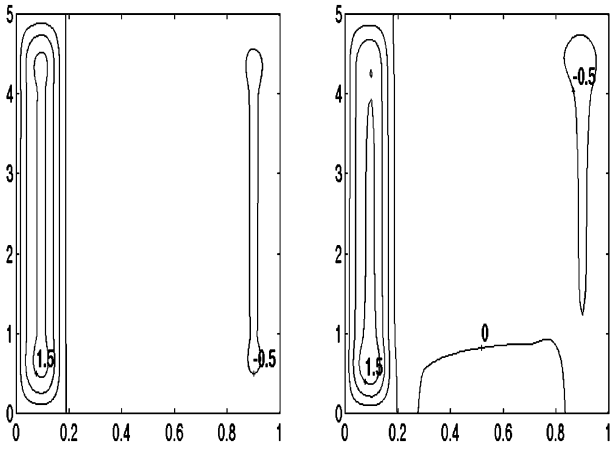


(a) $\Lambda$ Ra=$10^4$, Da=$10^{-4}$ (b) $\Lambda$ Ra=$10^5$, Da=$10^{-4}$

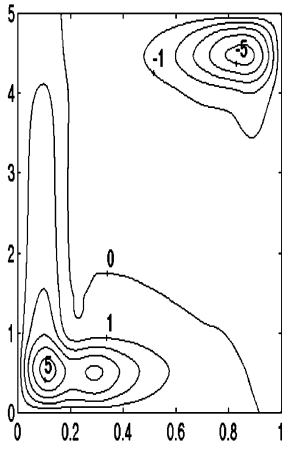


(c) $\Lambda$ Ra=$10^6$, Da=$10^{-4}$

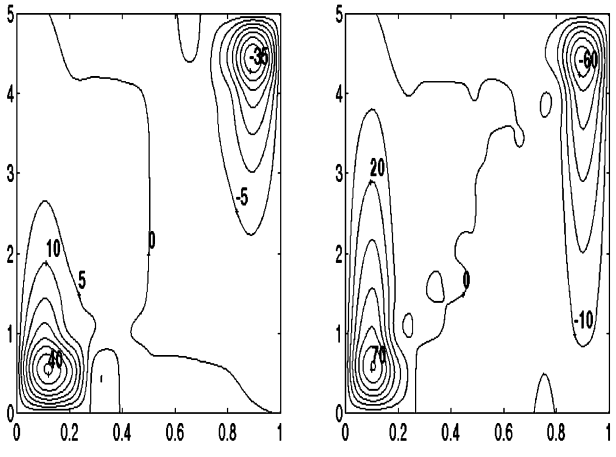


(d) $\Lambda$ Ra=$10^7$, Da=$10^{-4}$ (e) $\Lambda$ Ra=$10^8$, Da=$10^{-4}$

**Fig. 4.** Evaporation and condensation for different *Ra* number

Fig. 7 shows the combined effect considering *Da* and *Ra** numbers on $Nu_h$ number together. The shape of those curves is similar, which means for different *Da* number the influence of product *Ra*Da* on heat transfer rate is similar. We can also know from Fig. 7 that for lower *Da* number the heat transfer condition is better. But when *Da* number

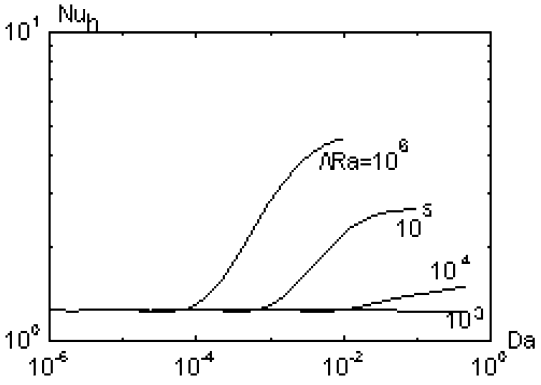


**Fig. 5.** Variation of average $Nu_h$ number with *Da* number for different *Ra* number

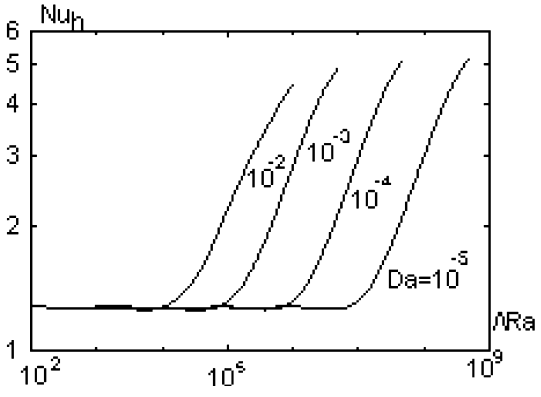


**Fig. 6.** Variation of average $Nu_h$ number with *Ra* number for different *Da* number

is rather small, its further decrease will bring little effect on $Nu_h$ number. For instance, in Fig. 7 the curves for *Da*=$10^{-4}$ and $10^{-5}$ are almost overlapped.

The model was calculated in the previous study involving water as fluid. The result is similar to the present one. Despite of the different physical properties for those two fluids, the tendency of physical quantity fields and the heat transfer characters for different *Da* number and *Ra* number are alike. However, the previous study is aimed to theoretical analysis and calculation. The actual one contains more consideration of practical application. In view of employment for the low grade solar energy, the selected working material should be able to have phase change under temperature 30 °C–60 °C at ordinary pressure. *R113* and *R30* are just fit for the requirement. And because of the differences between the two kinds of working fluids in physical property, not only the temperature of phase change and the working pressure in the media are different, but the soakage of liquid to the solid matrix is quite different. Thus, the some modifications in the numerical model are undertaken in the current calculation.

## 5 Conclusion

Natural convection and heat transfer through an enclosure with porous medium have been studied, which may guide the design of heat transfer enhancement for room heating.

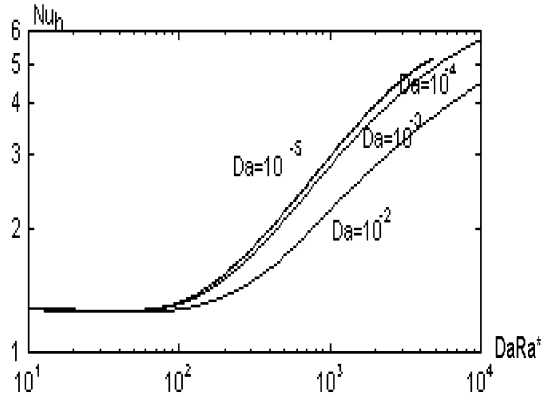


**Fig. 7.** Effect of *Da* number and *Ra* number on rate of heat transfer

(1) With the increase in *Ra* number of gaseous mixture in the enclosure, the isotherm lines twist gradually, and the streamlines change from symmetrical to asymmetrical patterns. These phenomena illustrate that the influence of natural convection is becoming more and more important. And when $Ra^*$ number approaches to the value of $10^8$, a relatively strong parallel flow is formed at the core of enclosure with the phase change of *R113*.

(2) By strengthening the flow in the enclosure, evaporation and condensation are more and more blooming. The bottom of the enclosure near the hot wall is where the biggest evaporation rate, whereas the biggest condensation rate is observed at the top near the cold wall. Thereby the steady natural convection and phase change is formed.

(3) Concerning the influence of *Da* and *Ra* numbers, we can divide the flow into three regimes: conductive, strongly Darcy-induced and weakly Darcy-induced regimes. In conduction regime, the natural convection has not been formed, and the heat transfer is mainly depended on conduction. For strongly Darcy-induced regime the heat transfer is enhanced quickly with the increase in *Da* number at a certain *Ra* number. But for weakly Darcy-induced regime the heat transfer enhancement is not strongly associated with Darcy mechanism, as *Da* number exerts very little influence on $Nu_h$ number. Those characters imply that the flow and the heat transfer are simultaneously related to Darcy, buoyancy and gravity mechanisms in the unsaturated porous media.

## References


1. Slattery, J.C., Two-phase flow through porous media. AIChE J. 16 (1970) 345–354
2. Whitaker, S., Simultaneous heat, mass and momentum transfer in porous media: a theory of drying, Advances in Heat Transfer, New York, Academic Press, 1977
3. Philip, J.R., DeVries, D.A., Moisture movement in porous materials under temperature gradients, Trans. Am. Geophys. Union, 38, 222–232 (1957)
4. DeVries, D.A., Simultaneous transfer of Heat and Moisture in Porous Media, Trans. Am. Geophys. Union, 39,909–916 (1958)
5. Udell, K.S., Heat transfer in porous media heated from above with evaporation, condensation and capillary effects, ASME J. Heat Transfer, 105 (1983) 485–492
6. Vafai, K., Tien, H.C., A numerical investigation of phase change effects in porous materials, Int. J. Heat Mass Transfer, 32 (1989) 1261–1277
7. Cheng, P., Pei, D.C.T., A mathematical model of drying process, Int. J. Heat and Mass Transfer, 32 (1989) 297–310
8. Gray, W.G., Hassanizadeh, S.M., Unsaturated flow theory including interfacial phenomena, Water Resour. Res, 27 (1991) 1855–1863
9. Bouddor, A., etc., Heat and mass transfer in wet porous media in presence of evaporation-condensation, Int. J. Heat and Mass Transfer, 41 (1998) 2263–2277
10. Zhao, T.S., Liao, Q., Cheng, P., Variations of buoyancy-induced mass flux from single-phase to two-phase flow in a vertical porous tube with constant heat flux, Journal of Heat Transfer, 121(1999) 646–652
11. Liao, Q., Zhao, T.S., A visual study of phase-change heat transfer in a two dimensional porous structure with a partial heating boundary, Int. J. Heat Mass Transfer, 43(2000) 1089–1102
12. Minkowyca, W.J., Haji-Sheikh, Vafai, K., On departure from local thermal equilibrium in porous media due to a rapidly changing heat source: the Sparrow number, Int. J. Heat and Mass Transfer, 42(1999) 3373–3385
13. Patrick Perre, Turner, I.W., A 3-D version of TransPore: a comprehensive heat and mass transfer computational model for simulation the drying of porous media, Int. J. Heat and Mass Transfer, 42(1999) 4501–4521
14. Liu, W., Zhao, X.X., Mizukami, K., 2D numerical simulation for simultaneous heat, water and gas migration in soil bed under different environmental conditions, Heat and Mass Transfer, 34(1998) 307–316
15. Liu, W., Zhao, X.X., Mizukami, K., Numerical Simulation of Heat and Mass Transfer in Soil, Proc. of the 10th Int. Symposium on Transport Phenomena, Japan, 1997
16. Liu, W., Peng, S.W., Mizukami, K., A general mathematical modeling for heat and mass transfer in unsaturated porous media: an application to free evaporative cooling, Heat and Mass Transfer, 31(1995) 49–55
17. Liu, W., Peng, S.W., Mizukami, K., Moisture Evaporation and Migration in Thin Porous Packed Bed Influenced by Ambient and Operative Conditions, Int. J. of Energy Research, 21(1997) 41–53
18. X.M. Huang, Liu, W., etc., Research on porous media with phase change in the building energy saving, Proc. of International Conference on Energy Conversion and Application, Wuhan, P.R. China, 2001